

# Finite element computational modeling of externally bonded CFRP composites flexural behavior in RC beams

André Luís Gamino<sup>†</sup>

*University of Campinas, 13083-852 Campinas, Brazil*

Túlio Nogueira Bittencourt<sup>‡</sup>

*University of São Paulo, 05508-900, São Paulo, Brazil*

José Luiz Antunes de Oliveira e Sousa<sup>‡†</sup>

*University of Campinas, 13083-852, Campinas, Brazil*

*(Received August 18, 2008, Accepted April 17, 2009)*

**Abstract** This paper focuses on the flexural behavior of RC beams externally strengthened with Carbon Fiber Reinforced Polymers (CFRP) fabric. A non-linear finite element (FE) analysis strategy is proposed to support the beam flexural behavior experimental analysis. A development system (QUEBRA2D/FEMOOP programs) has been used to accomplish the numerical simulation. Appropriate constitutive models for concrete, rebars, CFRP and bond-slip interfaces have been implemented and adjusted to represent the composite system behavior. Interface and truss finite elements have been implemented (discrete and embedded approaches) for the numerical representation of rebars, interfaces and composites.

**Keywords:** reinforced concrete; CFRP; non-linear finite element analysis; flexural strengthening.

---

## 1. Introduction

In the last years an increase has been observed in the fiber reinforced polymer (FRP) application for strengthening of reinforcement concrete structures. The excellent mechanical characteristics presented by these materials and their easy application introduced them into the structural strengthening field.

In Brazil, the application of such reinforcement systems is even more recent (Gamino and Bittencourt 2007a, Gamino *et al.* 2009). Although one may find a considerable number of successful applications, the technique is restricted and not well known due to the lack of technical information and the need of recommendations compatible with the national concrete structures codes.

---

<sup>†</sup> Ph. D., Corresponding Author, E-mail: [andre.gamino@gmail.com](mailto:andre.gamino@gmail.com)

<sup>‡</sup> E-mail: [tulio.bittencourt@poli.usp.br](mailto:tulio.bittencourt@poli.usp.br)

<sup>‡†</sup> E-mail: [jls@fec.unicamp.br](mailto:jls@fec.unicamp.br)

Herein, a strategy for modeling the flexural behavior of reinforced concrete strengthened beams is proposed, using the aforementioned two-dimensional programs under development. Experimental tests performed by the authors and other researchers have been used to validate the implementations and modeling.

## 2. Development programs

### 2.1. Pre and post-processor

QUEBRA2D program (Miranda and Meggiolaro 2003) comprises an interactive simulator of structural element damage processes, with a friendly user interface. It is a joint project under development by the Concrete Structures Modeling Group (GMEC), which involves the Brazilian Institutions: University of São Paulo, Pontifical Catholic University of Rio de Janeiro, and University of Campinas. All pre-processing has been performed in this program: domain representation, mesh generation, support conditions, loads, materials, and introduction of reinforcement steel bars and CFRP composites. Fig. 1 presents the program input and output screen.

### 2.2. Solver

FEMOOP Program (Martha and Menezes 1996) comprises a finite element solver for QUEBRA2D and has been developed on the paradigm of object oriented programming, using C++ language (Gamino

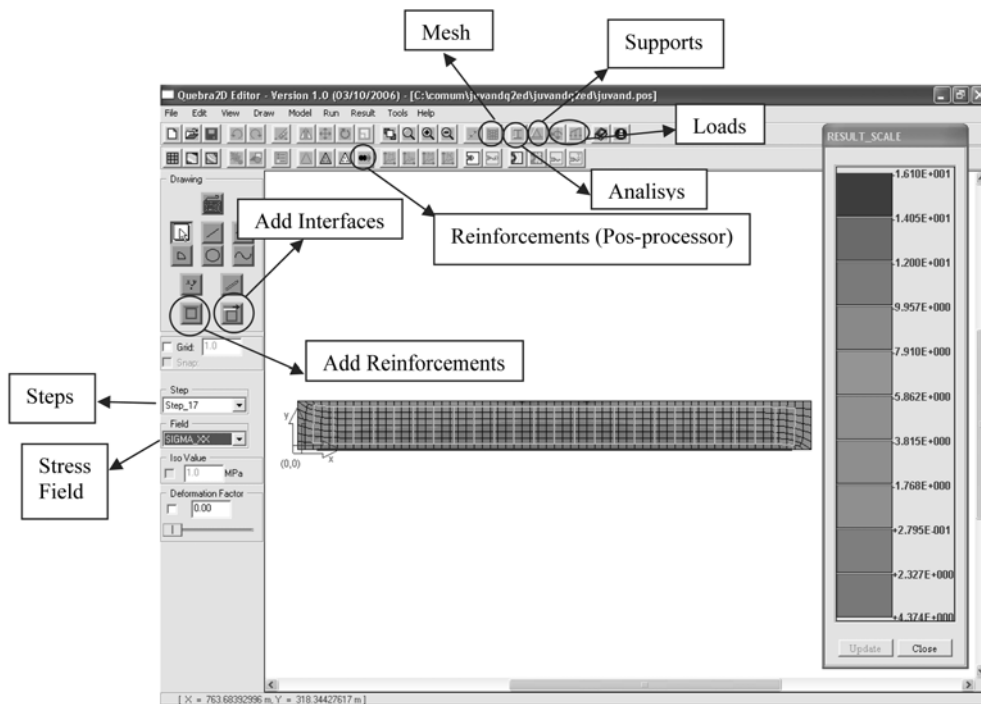


Fig. 1 QUEBRA2D Screen

and Bittencourt 2004, 2007b, Gamino *et al.* 2007).

Appropriate constitutive models for concrete, rebars, FRP and bond-slip interfaces have been implemented and adjusted to represent the composite system behavior. The interface and truss finite elements (linear, quadratic and cubic) have been implemented (discrete and embedded approaches) for the numerical representation of rebars, interfaces and composites.

### 3. Implemented finite elements

#### 3.1. Trusses

The implemented trusses elements (Fig. 2) for the representation of reinforcement bars, with two nodes (linear), three nodes (quadratic) and four nodes (cubic), can be found in Bathe (1996) or Kardestuncer and Norrie (1987). The strain-displacement matrix is:

$$B_s = \left[ \frac{\partial N_1}{\partial x} \frac{\partial N_1}{\partial y} \frac{\partial N_1}{\partial z} \cdots \frac{\partial N_n}{\partial x} \frac{\partial N_n}{\partial y} \frac{\partial N_n}{\partial z} \right] \quad (1)$$

where:

$$n=2 \text{ (linear), } n=3 \text{ (quadratic), } n=4 \text{ (cubic)}$$

The global stiffness matrix  $k$  for a concrete element with rebar, represented by  $nb$  embedded

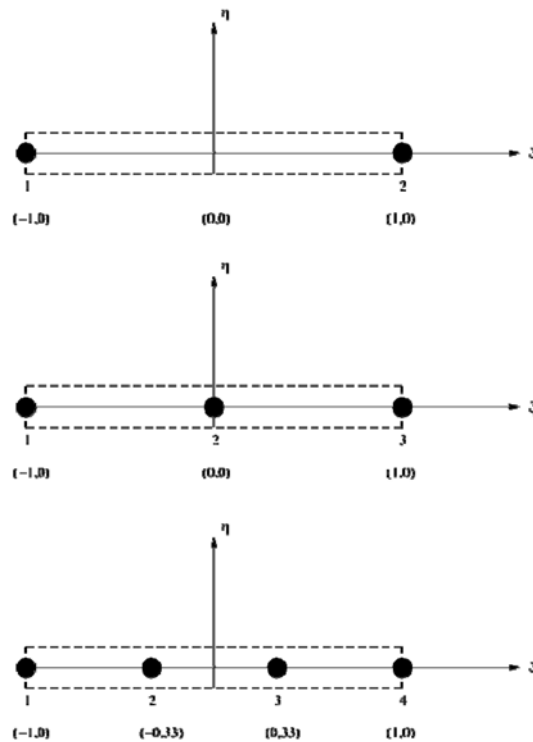


Fig. 2 Implemented trusses elements

elements crossing the parent element domain, can be obtained by:

$$k = k_c + \sum_{j=1}^{nb} k_{sj} \tag{2}$$

where:

- $k_c$  = concrete element stiffness matrix;
- $nb$  = number of rebars crossing the concrete element domain;
- $k_{sj}$  = steel reinforcement element stiffness matrix;

The steel reinforcement element stiffness matrix can be obtained by:

$$k_s = E_s A_s \int_s B_s B_s^T ds \tag{3}$$

where:

- $E_s$  = modulus of elasticity of the rebar steel;
- $A_s$  = cross section area of the rebar;

With the given points at the beginning and the end of the rebar, the intermediate points are obtained by:

$$\begin{Bmatrix} x \\ y \end{Bmatrix} = \sum_{j=1}^m \begin{bmatrix} H_j & 0 \\ 0 & H_j \end{bmatrix} \begin{Bmatrix} x_j \\ y_j \end{Bmatrix} \tag{4}$$

where:

- $H_j$  = interpolation function or shape function;
- $m$  = number of element nodes of the steel rebar;

The bar orientation for stiffness integration along the length  $ds$  is obtained using a mapping factor according to:

$$\frac{ds}{d\chi} = \sqrt{\left[\frac{dx}{d\chi}\right]^2 + \left[\frac{dy}{d\chi}\right]^2} \tag{5}$$

Elwi and Hrudehy (1989) proposed a solution for Eq. 4 using a Newton - Raphson algorithm. This

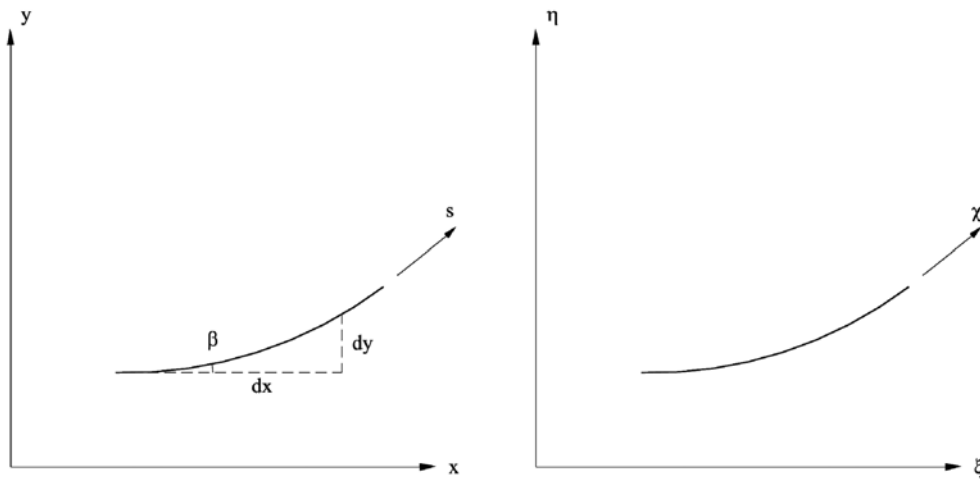


Fig. 3 Orientation for stiffness integration

solution consists in finding the roots for the vectorial equation:

$$\{f(\xi, \eta)\} = \begin{Bmatrix} x \\ y \end{Bmatrix} - \sum_{j=1}^m \begin{bmatrix} H_j & 0 \\ 0 & H_j \end{bmatrix} \begin{Bmatrix} x_j \\ y_j \end{Bmatrix} = 0 \tag{6}$$

The orientation for the stiffness integration is illustrated in Fig. 3. The final formulation using Elwi and Hrudehy (1989) model leads to:

$$\begin{Bmatrix} \frac{d\xi}{ds} \\ \frac{d\eta}{ds} \end{Bmatrix} = [J(\xi, \eta)]^{-1} \begin{Bmatrix} x_p - x_o \\ y_p - y_o \end{Bmatrix} \tag{7}$$

where:

- $x_o, y_o$  = rebar's local coordinates;
- $x_p, y_p$  = rebar's global coordinates;

### 3.2. Interfaces

The implemented elements (Fig. 4) for the interface representation can be found in Mehlhorn and Keuser (1986), using linear, quadratic and cubic shape functions. This isoparametric finite element type possesses finite dimension in the undeformed position but does not possess dimension in the traversal axis.

Considering two points  $i$  and  $k$  as in Fig. 4 the relative displacements can be written as:

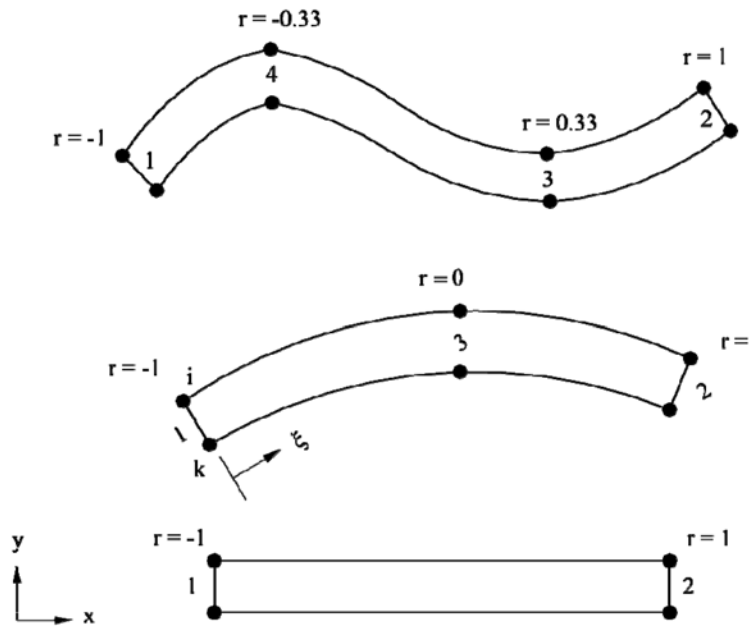


Fig. 4 Implemented interface elements

$$\begin{bmatrix} \Delta_x \\ \Delta_y \end{bmatrix} = \begin{bmatrix} -1 & 0 & 1 & 0 \\ 0 & -1 & 0 & 1 \end{bmatrix} \begin{bmatrix} u_i \\ v_i \\ u_k \\ v_k \end{bmatrix} \quad (8)$$

The nodal  $P$  stresses have been linked to bond stress  $\sigma$  as follows:

$$\begin{bmatrix} P_{xi} \\ P_{yi} \\ P_{xk} \\ P_{yk} \end{bmatrix} = \begin{bmatrix} -1 & 0 \\ 0 & -1 \\ 1 & 0 \\ 0 & 1 \end{bmatrix} \begin{bmatrix} \sigma_x \\ \sigma_y \end{bmatrix} \quad (9)$$

The relationship between the interface stress and the relative displacements in the local system of coordinates is given by the constitutive material law:

$$\begin{bmatrix} \sigma_\xi \\ \sigma_\eta \end{bmatrix} = \begin{bmatrix} C_{\xi\xi} & C_{\xi\eta} \\ C_{\eta\xi} & C_{\eta\eta} \end{bmatrix} \begin{bmatrix} \Delta_\xi \\ \Delta_\eta \end{bmatrix} \quad (10)$$

where:

- $C_{\xi\xi}$  = bond modulus in  $\xi$  direction;
- $C_{\eta\eta}$  = bond modulus in  $\eta$  direction;

Finally the stiffness matrix can be obtained by using:

$$k = \int_A B^T C^{gl} B \, dA \quad (11)$$

The global constitutive matrix  $C^{gl}$  is:

$$C^{gl} = T^T . C . T \quad (12)$$

## 4. Implemented materials

### 4.1. Uncracked concrete

Ottosen (1977) criterion can be used for representing the concrete integrity. The rupture surface can be written as:

$$F = A \frac{J_2}{f_{cm}^2} + \lambda \frac{\sqrt{J_2}}{f_{cm}} + B \frac{I_1}{f_{cm}} - 1 = 0 \quad (13)$$

where:

- $A, B$  = material parameters;
- $f_{cm}$  = average concrete strength in compression;
- $J_2$  = second invariant of deviatoric stress tensor;
- $I_1$  = first invariant of stress tensor;

The  $\lambda$  factor determinates the stress meridian:

$$\lambda = K_1 \cos \left[ \frac{1}{3} \cos^{-1} (K_2 \cos(3\theta)) \right] \text{ for } \cos(3\theta) \geq 0 \quad (14)$$

$$\lambda = K_1 \cos \left[ \frac{\pi}{3} - \frac{1}{3} \cos^{-1} (-K_2 \cos(3\theta)) \right] \text{ for } \cos(3\theta) < 0 \quad (15)$$

where  $K_1$  and  $K_2$  are material parameters;

By using three-invariant system, the rupture surface is:

$$F(I_1, J_2, \cos(3\theta)) = 0 \quad (16)$$

and the angular invariant  $\cos(3\theta)$  is:

$$\cos(3\theta) = \frac{3\sqrt{3} J_3}{2 J_2^{3/2}} \quad (17)$$

where  $J_3$  is the third invariant of the deviatoric stress tensor;

Using the expressions by Dahl (1992) the material factors can be found by using the concrete tension/compression strength relation:

$$\begin{aligned} K &= f_{cm}/f_{cm} \\ A &= \frac{1}{9K^{1.4}} \quad B = \frac{1}{3.7K^{1.1}} \\ K_1 &= \frac{1}{0.7K^{0.9}} \quad K_2 = 1 - 6.8(K - 0.07)^2 \end{aligned} \quad (18)$$

Dahl (1992) gave recommendations where the four Ottosen parameters can be computed by knowing only the compressive strength. He claims that the model is able to serve as a failure surface for normal and high strength concrete with parameters in according to Hartl (2002).

Plasticity models can be used in FEMOOP Program to simulate the concrete behavior. In this case, an algorithm of elastoplastic return proposed by Crisfield (1997) and Owen and Hinton (1980) can be used. When a tension state is located out of the rupture surface, this return algorithm is applied to restore the tension levels to the functional surface.

#### 4.2. Cracked concrete

Coupled with the model of physical integrity, a model of rotating smeared crack was implemented. The cracking criterion compares the tensile stresses (from Ottosen's model 1977) in the Gauss points with the material tensile strength. After the onset of the first crack, a linear softening model was used (Fig. 5).

Using a linear softening model in tension, the crack opening can be obtained through:

$$w^{cr} = \frac{2G_f}{f_t}; \text{ or } w^{cr} = \varepsilon^{cr} . h \quad (19)$$

where:

$w^{cr}$  = crack width;

$G_f$  = fracture energy in mode I;

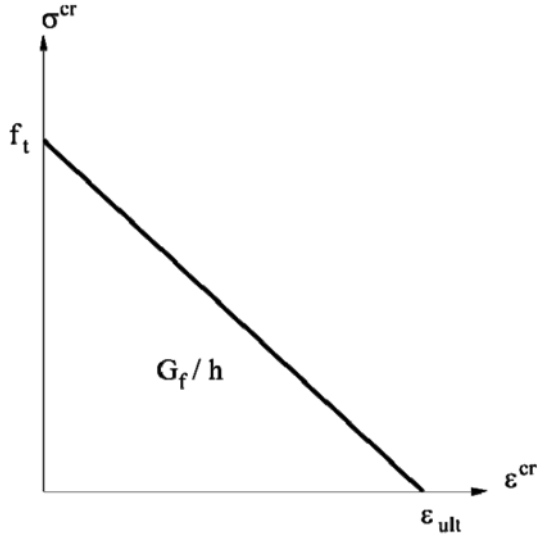


Fig. 5 Linear softening model

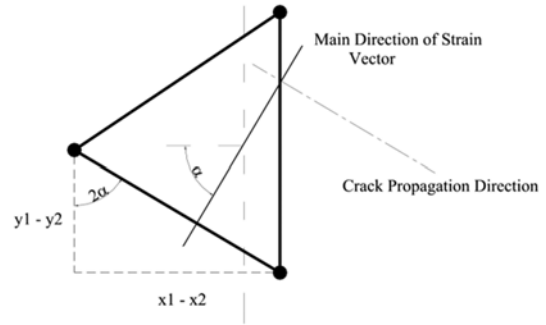


Fig. 6 Crack propagation direction

$\varepsilon^{cr}$  = crack strain;

$h$  = crack band width;

The crack opening displacements were computed from the crack strains, which depend on the failure models adopted for the concrete and the steel reinforcement. The used reinforcement ratios influence the stress level in the tensile portion of the structure, and thus the crack opening displacements. Therefore, crack opening displacements decrease as the reinforcement ratio increases. Crack opening displacements depend also on the tension-softening model adopted.

The deformations in concrete can be obtained through:

$$\varepsilon = \varepsilon_e + \varepsilon^{cr} \tag{20}$$

where:

$\varepsilon_e$  = elastic strain vector obtained from elastic matrix;

$\varepsilon^{cr}$  = crack strain vector obtained from the contribution of the concrete's degradation process;

The contribution of the cracks on the strain vector depends exclusively on the computed crack opening and the finite element area (Fig. 6):

$$\begin{Bmatrix} \varepsilon_x \\ \varepsilon_y \\ \gamma_{xy} \end{Bmatrix} = \begin{Bmatrix} 1 \\ -\nu \\ 0 \end{Bmatrix} \sigma/E + \begin{Bmatrix} y_1 - y_2 \\ 0 \\ x_2 - x_1 \end{Bmatrix} w^{cr}/2A \tag{21}$$

where:

$A$  = finite element area;

The angle  $\alpha$  in Fig. 6 indicates the direction of the principal strain vector. Crack propagates in the perpendicularly to this direction (Jirásek and Zimmermann 1998):

$$\alpha = \lim_{w^{cr} \rightarrow \infty} 1/2 \arctan \frac{\gamma_{xy}}{\varepsilon_x - \varepsilon_y} = 1/2 \arctan \frac{x_2 - x_1}{y_1 - y_2} \tag{22}$$

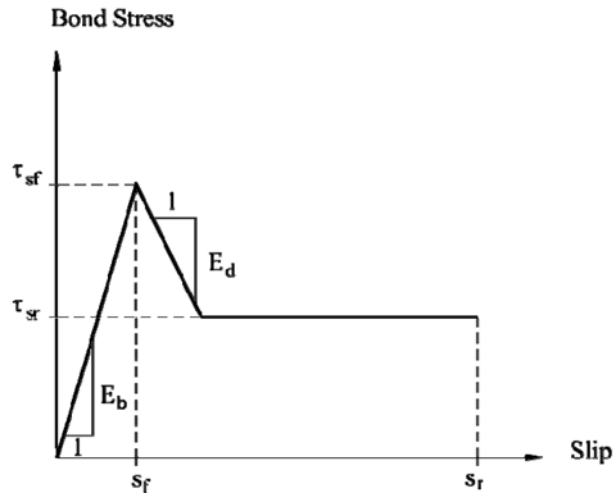


Fig. 7 Homayoun and Mitchell (1996) bond-slip law

In the smeared crack models, the strong discontinuity associated with the crack is spread throughout the finite element. As well known, the continuity of the displacement field assumed for these models is not compatible with the actual discontinuity. Despite this, this type of models has been extensively used due to its computational simplicity provided by treating cracks in a continuum framework, as well as to the good predictions of structural behavior of reinforced concrete members reported in the literature.

#### 4.3. Bond-slip law

Homayoun and Mitchell (1996) multilinear bond-slip model described in Fig. 7 has been implemented for the interfaces behavior representation. The model requires the following parameters:

- $\tau_{sf}$  = the interface bond strength,
- $\tau_{sr}$  = the interface residual bond strength,
- $s_f$  = the interface slip in rupture,
- $s_r$  = the residual interface slip,
- $E_b$  = the pre-peak bond modulus
- $E_d$  = the post-peak bond modulus.

## 5. Computational modeling

Tables 1 to 4 present the properties of materials, concrete, steel, carbon fiber and epoxy resin, used to model the beam. Table 5 presents the non-linear analysis parameters used in every beam.

### 5.1. Araújo beams

The V4 beam by Araújo (2002) shown in Fig. 8 has been used to model a flexure strengthened beam. The Fig. 9-a shows the load-displacement curves and Fig. 9-b shows the load-axial strain

Table 1 Concrete mechanical properties used for beam modeling

Property	Araújo (2002)	Gamino (2007)	Juvandes (1999)
E [MPa]	30,000	40,000	42,200
$\nu$	0.15	0.15	0.15
A	1.61	1.96	1.82
B	3.23	3.28	3.26
$f'_c$ [MPa]	29.1	45.0	38.1
$K_1$	11.65	11.55	11.59
$K_2$	0.984	0.988	0.986
$\beta$	0.01	0.05	0.01
$f_t$ [MPa]	2.9	4.5	2.9
$G_f$ [N/mm]	0.012	0.015	0.028
Crack Band Width [mm]	8.10	14.65	21.65
Constitutive Model	Ottosen	Ottosen	Ottosen

Table 2 Reinforced bars mechanical properties used for beam modeling

Property	Araújo (2002)	Gamino (2007)	Juvandes (1999)
E [MPa]	210,000	205,000	174,000 195,000 (traction rebars)
$\nu$	0.30	0.30	0.30
$f_y$ [MPa]: Strength Rebar	858.0	640.0	497.1
Bottom Reinforcement	568.0	640.0	192.3
Stirrup	642.0	640.0	192.3
$A_s$ : Strength Rebar	2 $\phi$ 5 mm	2 $\phi$ 6.3 mm	2 $\phi$ 3 mm
Bottom Reinforcement	3 $\phi$ 12.5 mm	2 $\phi$ 6.3 mm	3 $\phi$ 8 mm
Stirrup	$\phi$ 6.3 mm at 100 mm	$\phi$ 6.3 mm at 60 mm	$\phi$ 3 mm at 60 mm
Constitutive Model	von Mises	von Mises	von Mises
Concrete-steel Interface Parameters			
Bond Stress [MPa]	12	12	12
Residual Bond Stress [MPa]	6.0	6.0	6.0
Slip in Rupture [mm]	0.3	0.3	0.3
Residual Slip [mm]	0.9	0.9	0.9
Pre-Peak Bond Module [MPa]	40,000	40,000	40,000
Post-Peak Bond Module [MPa]	20,000	20,000	20,000
Bond Model	Homayoun	Homayoun	Homayoun

Table 3 CFRP mechanical properties used for beam modeling

Property	Araújo (2002)	Gamino (2007)	Juvandes (1999)
Elasticity Module [MPa]	235,000	230,000	165,000
Poisson's Coefficient	0.25	0.25	0.25
Rupture Stress [MPa]	---	3,500	---
Constitutive Model	isotropic	von Mises	isotropic

Table 4 Epoxy resins mechanical properties used for beam modeling

Property	Araújo (2002)	Gamino (2007)	Juvandes (1999)
Bond Stress [MPa]	1.5	12	3.0
Residual Bond stress [MPa]	1.0	1.5	1.5
Interface Slip in Rupture [mm]	0.6	0.6	0.6
Residual Interface Slip [mm]	0.9	0.9	0.9
Pre – Peak Bond Module [MPa]	3.034	3,800	12,800
Post – Peak Bond Module [MPa]	1,500	1,900	6,400
Bond Model	Homayoun	Homayoun	Homayoun

Table 5 Non-linear analysis parameters for the modeled beams

Tested Beam	Number of Finite Elements	Time of Processing (sec)	Tolerance	Analysis Algorithm	Convergence Criterion
Araújo (2002)	1,058	150	0.035	NRM	Forces Control
Gamino (2007)	1,750	270	0.040	NRM	Forces Control
Juvandes (1999)	1,164	192	0.035	NRM	Forces Control

Observation: NRM represents the Newton-Raphson Modified algorithm.

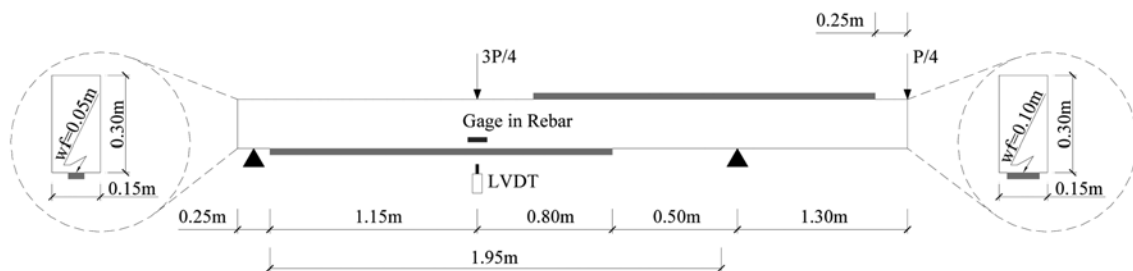


Fig. 8 Test setup for the strengthened beams tested by Araújo (2002)

curves (experimental and numerical) corresponding to the steel bottom reinforcement and Fig. 10 shows the crack pattern obtained from the implemented rotating smeared crack model. The first cracks have been numerically obtained for a 88.2 kN total load and the computed maximum crack width was 0.24 mm; in the physical tests these values were respectively 90 kN and 0.20 mm.

### 5.2. Gamino beams

The series of rectangular beams strengthened using CFRP composites tested by the authors (Gamino 2007) have been modeled using this proposed numerical strategy. The beam model is shown in Fig. 11. One CFRP layer has been used for the beam flexural strengthening.

This beam has been modeled using discrete and embedded reinforcements, with and without a bond-slip model. The obtained load-displacement curves are shown in Fig. 12.

The responses using embedded reinforcements resulted more stiff in comparison to the discrete approach. Using a bond-slip law, the numerical curves were closer to experimental curve. However the best results were obtained using embedded reinforcements with debonding effect.

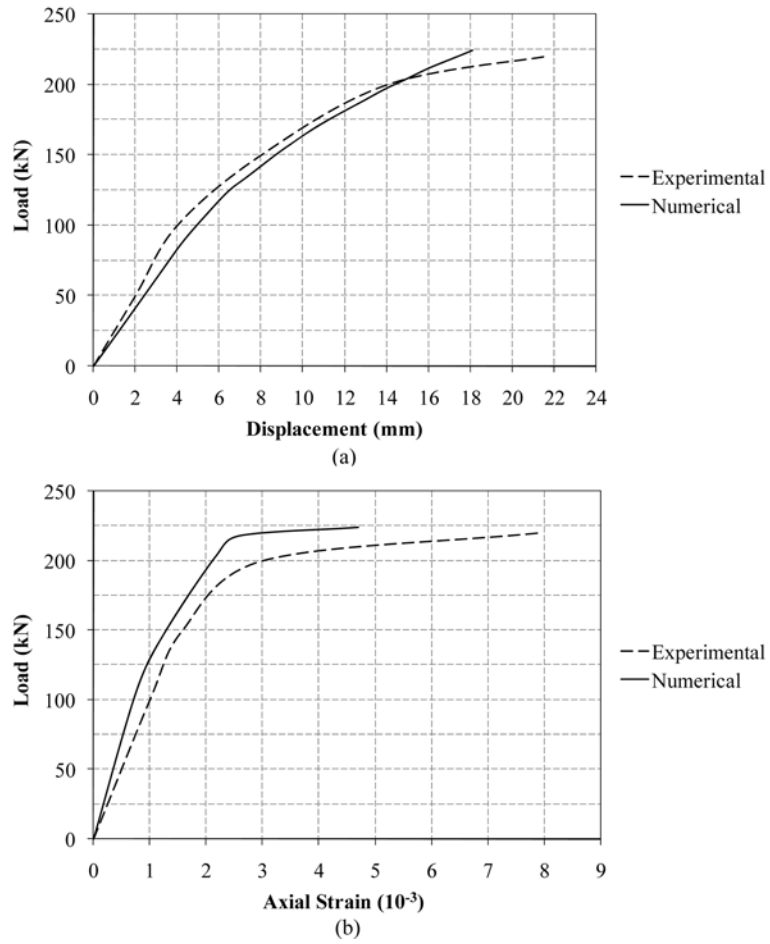


Fig. 9 Load-displacement curve (a) and load-axial strain curve to bottom reinforcement steel (b) obtained for V4 beam by Araújo (2002)

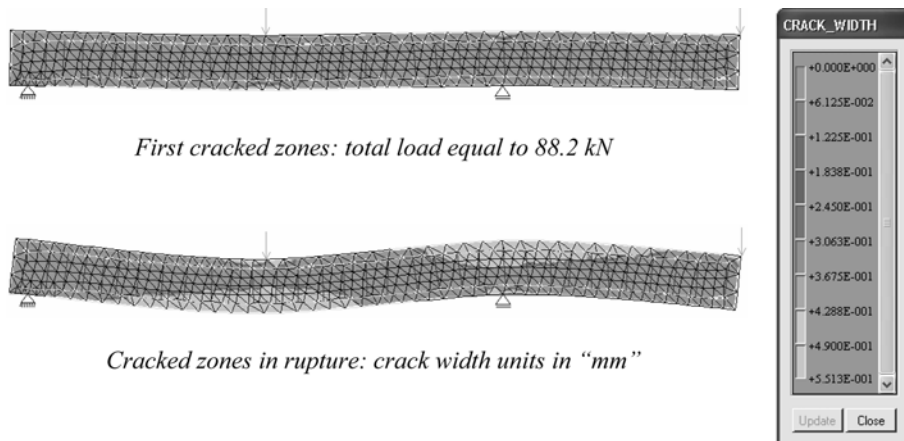


Fig. 10 Numerical crack pattern obtained for V4 beam by Araújo (2002)

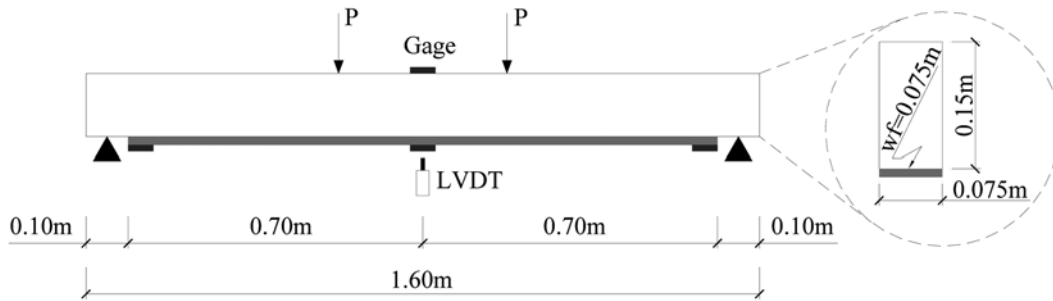


Fig. 11 Test setup for the strengthened beams tested by Gamino (2007)

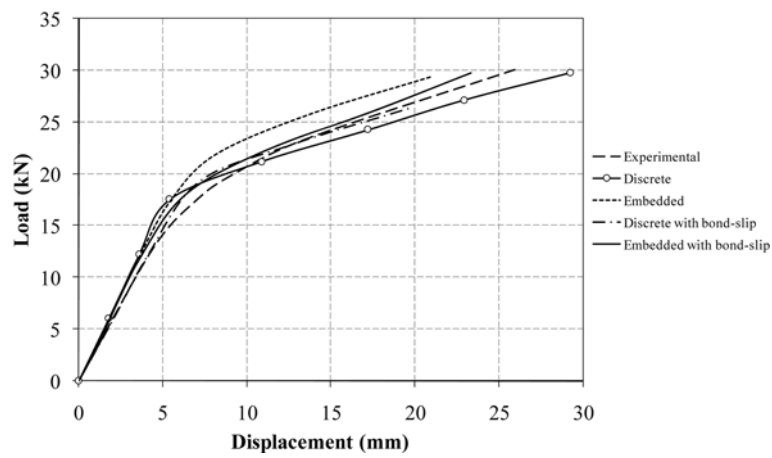


Fig. 12 Load-displacement curves obtained for beams tested by Gamino (2007)

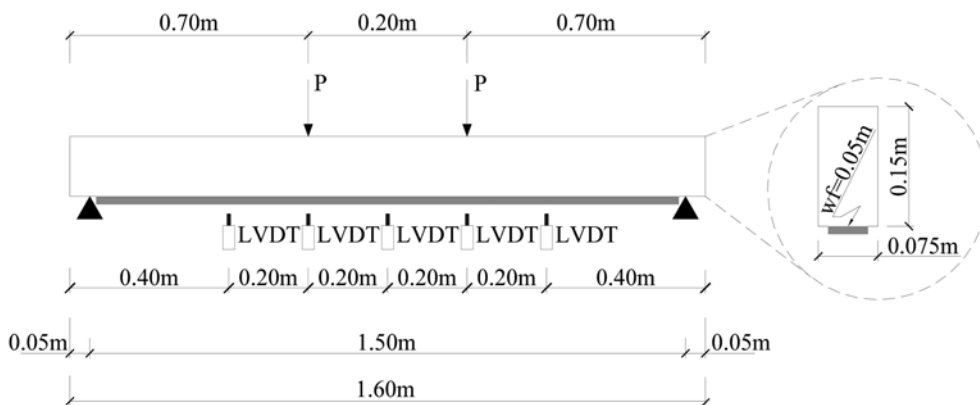


Fig. 13 Test setup for the strengthened beams tested by Juvandes (1999)

### 5.3. Juvandes beams

The B3 beam tested by Juvandes (1999) in a four-point load setup has been modeled. The modeled beam shows in Fig. 13.

Fig. 14 shows the load-displacement curves and Fig. 15 shows the stress field in reinforcements

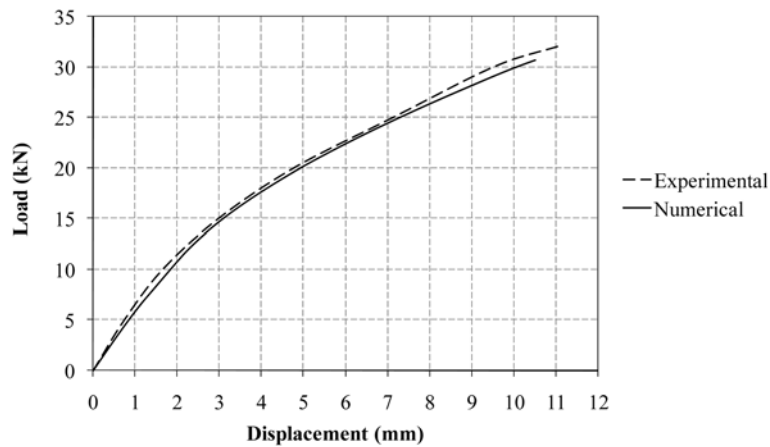


Fig. 14 Load-displacement curves (LVDT in mid-span) obtained for B3 beam tested by Juvandes (1999)

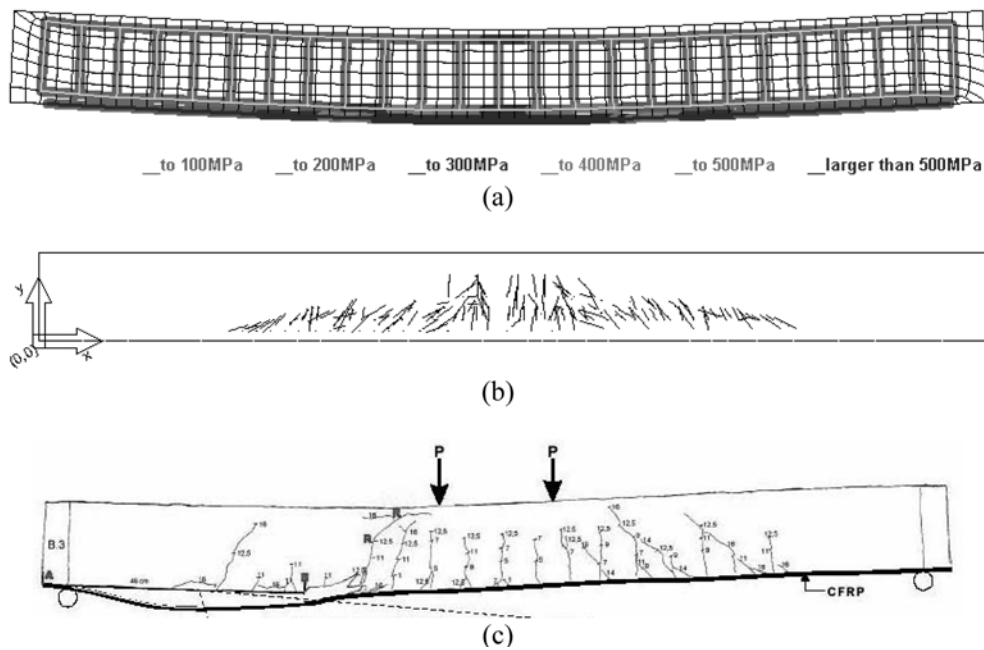


Fig. 15 Stress field in rebars/composites (a), numerical crack patterns (b) and experimental crack patterns (c) obtained for B3 beam tested by Juvandes (1999)

and crack pattern. The maximum strain in CFRP and the maximum shear stress in the epoxy resin obtained in numerical simulations are respectively 0.83% and 3.37 MPa. The corresponding values from the physical test are respectively 0.62% and 5.02 MPa.

The rupture mechanism detected in the experimental tests was a peeling caused by wider flexure crack. This mechanism was not detected in the numerical analysis (this is a hard-to-capture phenomenon). With these results the FE models and implementations have been validated in a global and in a local scale.

## 6. Conclusions

This paper focuses on the flexural behavior of RC beams externally strengthened with a Carbon Fiber Reinforced Plastics (CFRP) fabric. A non-linear finite element (FE) modeling strategy is proposed to support the experimental analysis of the flexural behavior of the beams. The following conclusions result from the performed numerical modeling :

- The implemented smeared rotating crack model produces good results for Araújo's (2002) beam; Numerical modeling indicated the first cracks when the total load was 88.2 kN, and maximum crack with was 0.24 mm. The corresponding values from the experimental tests were, respectively, 90 kN and 0.20 mm.
- In Gamino's (2007) beam the responses obtained with embedded reinforcements presented higher stiffness in comparison to the discrete approach. Using the bond-slip law, the numerical curves were closer to the experimental curve, and the best results were obtained using embedded reinforcements with debonding effect.
- In Juvandes' (1999) beam modeling the maximum strain in CFRP and the maximum shear stress in epoxy resin obtained in numerical simulations are respectively 0.83% and 3.37 MPa. The corresponding values in the experimental test were, respectively, 0.62% and 5.02 MPa.
- With these results, the proposed finite element modeling were validated in a global and in a local scale.

## Acknowledgements

The authors wish to express their gratitude and appreciation to FAPESP-Research Support Foundation of São Paulo State (Processes 06/05843-2 and 04/03049-1) and to CNPq-Scientific and Technological Development National Board (Processes 304915/2005-0 and 307051/2006-4) for financial support to this research.

## References

- Araújo, A.C.N. (2002), *Experimental study of RC beams strengthened with CFRP's composites*, MSc Thesis (in Portuguese), Pontifícia Universidade Católica do Rio de Janeiro, Rio de Janeiro.
- Bathe, K.J. (1996), *Finite Element Procedures*, Prentice Hall, Englewood Cliffs.
- Crisfield, M.A. (1997), *Non-Linear Finite Element Analysis of Solids and Structures*, John Wiley & Sons.
- Dahl, K.K.B. (1992), *A failure criterion for normal and high strength concrete*, Technical University of Denmark, Lyngby.
- Elwi, A.E. and Hrudey, T.M. (1989), "Finite element model for curved embedded reinforcement", *J. Eng. Mech.*, **115**(4), 740-754.
- Gamino, A.L. (2007), *Physical and computational modeling of RC structures strengthened with FRP*, PhD Thesis (in portuguese), Escola Politécnica, Universidade de São Paulo, São Paulo.
- Gamino, A.L., Bittencourt, T.N. and Sousa, J.L.A.O. (2007), "Numerical modeling of classic concrete beam tests", *Struct. J.*, IBRACON **3**(2), 201-229.
- Gamino, A.L. and Bittencourt, T.N. (2007a), "Reinforced Concrete Beams Strengthened with CFRP: Experimental, Analytical and Numerical Approaches", *Proceedings of the 8th International Symposium on Fiber Reinforced Polymer Reinforcement for Concrete Structures - FRPRCS-8*, Patras, **1**, 130-131.
- Gamino, A.L. and Bittencourt, T.N. (2007b), "Numerical Evaluation of Plastic Rotation Capacity in Reinforced-

- Concrete Beams”, *Proceedings of the 6th International Conference on Fracture Mechanics of Concrete and Concrete Structures - FraMCoS 6*, Catania, **2**, 665-670.
- Gamino, A.L. and Bittencourt, T.N. (2004), *High Performance Finite Elements and Their Applications*. Tsinghua University Press, **2**, 25.
- Gamino, A.L., Sousa, J.L.A.O. and Bittencourt, T.N. (2009), “Application of carbon fiber reinforced polymer in strengthening to shear R/C T Beams”, *Proceedings of the 9th International Symposium on Fiber Reinforced Polymer Reinforcement for Concrete Structures - FRPRCS-9*, Sydney (in Press).
- Hartl, H. (2002), *Development of a continuum-mechanics-based for 3D finite element analysis of reinforced concrete structures and application to problems of soil-structure interaction*, PhD Thesis, Technische Universität Graz, Austria.
- Homayoun, H.A. and Mitchell, D. (1996), “Analysis of bond stress distributions in pullout specimens”, *J. Struct. Eng.*, **122**(3), 255-261.
- Jirásek, M. and Zimmermann, T. (1998), “Analysis of rotating crack model”, *J. Eng. Mech. ASCE*, **74**, 842-851.
- Juvandes, L.F.P. (1999), *Reforço e reabilitação de estruturas de betão usando materiais compósitos de CFRP*. PhD Thesis (in portuguese), Faculdade de Engenharia, Universidade do Porto, Porto.
- Kardstuncker, H. and Norrie, D.H. (1987), *Finite Element Handbook*, McGraw-Hill.
- Martha, L.F., Menezes, I., Lages, E.N., Parente Jr. E., and Pitangueira, R. (1996), “An oop class organization for materially nonlinear finite element analysis”, *Proceedings of Joint Conference of Italian Group of Computational Mechanics and Ibero-Latin American Association of Computational Methods in Engineering*, Padova, 229-232.
- Mehlhorn, G. and Keuser, M. (1986), *Finite element analysis of reinforced concrete structures*, Prentice Hall, Englewood Cliffs.
- Miranda, A.C.O., Meggiolaro, M.A., Castro, J.T.P., Martha, L.F., and Bittencourt, T.N. (2003), “Fatigue Life and Crack Path Predictions in Generic 2D Structural Components”, *Eng. Fract. Mech.*, **70**(10), 1259-1279.
- Ottosen, N.S. (1977), “A failure criterion for concrete”, *J. Eng. Mech. Div.*, **103**(4), 527-535.
- Owen, D.R.J. and Hinton, E. (1980), *Finite Elements in Plasticity – Theory and Practice*, Pineridge Press.